Supplemental Material: Semi-Dirac transport and anisotropic localization in polariton honeycomb lattices

B. Real,[1] O. Jamadi,[1] M. Milićević,[2] N. Pernet,[2] P. St-Jean,[2] T. Ozawa,[3,4] G. Montambaux,[5]
I. Sagnes,[2] A. Lemaître,[2] L. Le Gratiet,[2] A. Harouri,[2] S. Ravets,[2] J. Bloch,[2] and A. Amo[1]

[1] *Univ. Lille, CNRS, UMR 8523 – PhLAM – Physique des Lasers Atomes et Molécules, F-59000 Lille, France*
[2] *Centre de Nanosciences et de Nanotechnologies (C2N), CNRS - Université Paris-Sud/Paris-Saclay, Palaiseau, France*
[3] *Advanced Institute for Materials Research, Tohoku University, Sendai 980-8577, Japan*
[4] *Interdisciplinary Theoretical and Mathematical Sciences Program (iTHEMS), RIKEN, Wako, Saitama 351-0198, Japan*
[5] *Laboratoire de Physique des Solides, CNRS, Université Paris-Sud, Université Paris-Saclay, 91405 Orsay Cedex, France*

(Dated: July 17, 2020)

SETUP AND EXPERIMENTAL CONDITIONS

The experiments reported in the main text are done using the experimental setup schematized in Fig. 1(a). The experiments are carried out at low temperature (10 K) by placing the sample (lattices of semiconductor micropillars) in a closed-cycle cryostat. We excite non resonantly the lattices by using a linearly polarized beam coming from a continuous-wave monomode Ti:Sapphire laser at 745 nm. After traveling through a polarization-maintaining monomode optical fiber, the beam shows a clear gaussian profile. From there, the beam is driven to the cryostat where it is tightly focused on the lattices by an aspherical lens of 8-mm focal length (NA= 0.45) [f_1 in Fig. 1(a)]. The absorption of the laser by the semiconductor creates a hot cloud of electron-hole pairs that incoherently relax and populate all the polaritonic bands of the structure. Since polaritons have a finite lifetime (12-14 ps) they leak

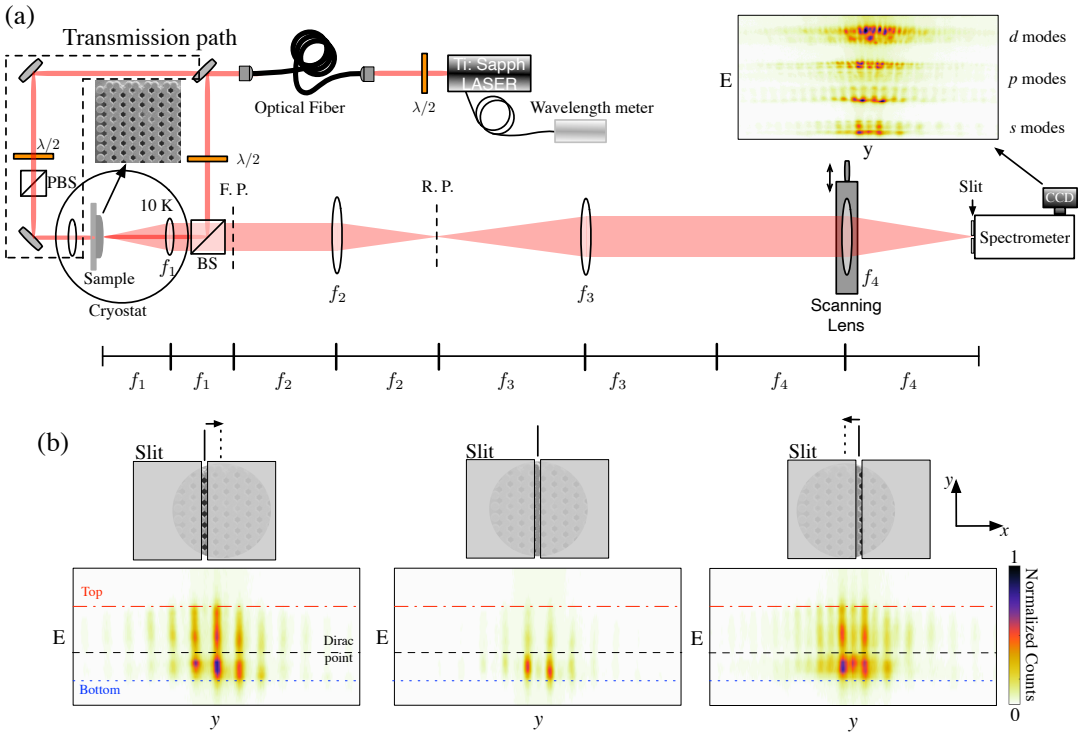

FIG. 1. (a) Scheme of the experimental setup to measure the polariton emission at a given energy. The region in the dashed rectangle shows the beam path for transmission experiments. (b) The upper row depicts selected regions of the image of the lattice by a slit at three different horizontal (x) positions. The lower row presents the population of polaritons as a function of the energy (E) and the real space along vertical (y) direction for the respective horizontal positions. Dotted, dashed and dot-dashed lines respectively point out the bottom, Dirac-point and top energy of the s bands.

out the cavity in the form of photons that encode the energy and momentum of the polaritons inside the structure. This photoluminescence is collected by the same 8-mm lens used for the excitation and an image system generates a 120-times magnified image of the lattice at the entrance port of a spectrometer. The entrance slit of the spectrometer, and a scanning lens placed on a motorized translation stage [see Fig. 1(a)] allow selecting the real space image of a vertical slice of the emission. The slit has a width of $\sim 32.5\,\mu$m which, taking into account the magnification of the set-up, corresponds to $0.3\,\mu$m on the sample [see Fig. 1(b) upper row]. This 1D y-slice of the image is dispersed by the spectrometer and imaged on a CCD. The image of the CCD, shown in Fig. 1(b) lower row, represents y position in one direction and energy on the other. Thus, the energy-resolved emission from the polariton bands can be recorded along y direction for a specific x position. Using the motorized-translation stage, the position of the scanning lens can be shifted in the x direction such that the emission from different x positions on the lattice can be recorded. From all the recorded spectra, real space images of the emission at any given energy can be reconstructed. The energy precision is given by the pixel resolution of the CCD, being $33.1\,\mu$eV.

Additionally, we also perform an angle-resolved scan of the momentum space by removing f_3 lens. By doing so, the imaging system formed by the f_2 lens and the scanning lens images the Fourier plane of f_1 on the entrance port of the CCD. Each point in this plane corresponds to an angle of emission of the sample θ, which is directly related to the in-plane momentum of polaritons $k_|$ via $k_| = k_0 \cos(\theta)$, where k_0 is the total momentum of the out coming photon. This configuration of the imaging system allows us to observe the band structure for given cuts of the Fourier plane as shown in Fig. 1 of the main text. Therefore, we can both image the momentum and real space of the emission.

To perform resonant experiments, we set the wavelength of the laser to the (semi-)Dirac-point energy with the help of a wavelength meter. The energy of the (semi-)Dirac point is obtained from the spectra recorded in the non-resonant experiment described above. Once the wavelength is set, we focalise the laser spot on one pillar [A or B Fig. 1(a) main text], with FWHM of $\approx 2\,\mu$m. To prevent the intense reflected laser beam from reaching the CCD and, thus, be able to record the emission from the injected polaritons [Fig. 3(a) and (c) main text], we place a spatial filter in the first real plane (R.P.) shown in Fig. 1(a). The effective size of the spatial filter corresponds to the white central area in Fig. 3(a) and (c) of the main text.

ANISOTROPIC EMISSION FROM VACANCY-LIKE POLARITON DISTRIBUTION

Figure 3 of the main text presents the emission when exciting a lattice with $\beta = 2$ at the semi-Dirac cone energy (E_0) on a single pillar. As discussed in the main text, the interference between the excitation field the polariton

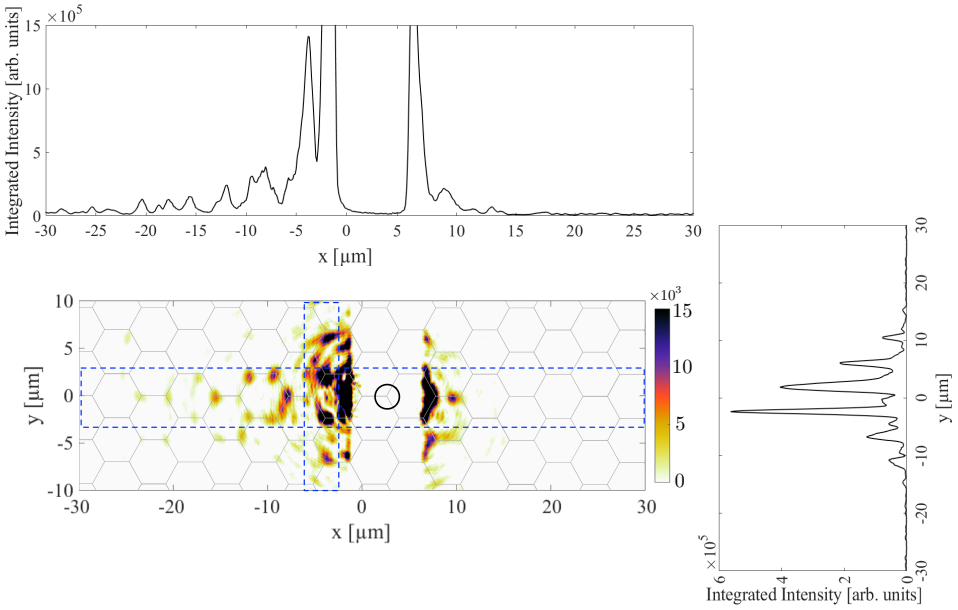

FIG. 2. The central panel shows Fig. 3(c) of the main text in linear color scale. The circle points out the pumped pillar. Top panel shows a vertical integrated plot along the x direction, while the right panel shows a horizontal integrated plot along the y direction. Enclosed regions depict the integrated areas.

emission results in a near-zero field amplitude at the pillar on which the laser is focused, resulting in the analog of a bulk vacancy. Reference [1] predicted that vacancy states at E_0 should be strongly asymmetric, as clearly seen in Fig. 3 of the main text, which is displayed in logarithmic scale. To provide further support to these observations, the central panel of Fig. 2 shows in linear color scale the data displayed in Fig. 3(c) of the main text, under steady-state excitation of a B site. The directionality of the decay of the emission is further evidenced in the horizontal and vertical profiles shown in the upper and right panels. They show the emitted intensity integrated along the vertical (upper panel) and horizontal (right panel) direction within the dashed rectangles depicted in the central panel. Along the x direction, the integrated profile clearly presents a much longer decay towards negative values. Conversely, the right panel exhibits a symmetric and fast decay in the y direction. Along this direction we expect the polariton distribution to cover only one hexagon (simulated images in Fig. 3 of the main text). However, scattered light of the reflected pumped beam is also present at longer distances.

VACANCY STATES IN REGULAR HONEYCOMB LATTICES ($\beta = 1$)

We have also explored the formation of vacancy-like states in the bulk of regular honeycomb lattices with $\beta = 1$. For this purpose, we fabricate a planar semiconductor microcavity made of 28 (top) and 32 (bottom) pairs of $\lambda/4$ alternating layers of $Ga_{0.10}Al_{0.90}As$ and $Ga_{0.05}Al_{0.95}As$ ($\lambda = 880$ nm), a λ spacer of GaAs, and a single 20-nm-width $In_{0.09}Ga_{0.91}As$ quantum well at the center of the cavity. This microcavity is etched down to the substrate into honeycomb lattices of coupled micropillars of 2.75 μm, with a center-to-center distance of 2.4 μm. At cryogenic temperature the lattices possess a Rabi splitting of 3.5 meV. The $In_{0.09}Ga_{0.91}As$ quantum well used in this microcavity sample allows for experiments in transmission geometry, in which the resonant excitation beam impinges on the sample on one side and observation is done from the other side [the excitation beam follows the path of the enclosed region in Fig. 1(a)]. Fig. 3(a) presents the measured intensity in logarithmic scale when a laser at the Dirac-point energy ($E_0 = 1402.54$ meV) is focused on a single micropillar of the A sublattice (marked with a circle). The intensity distribution decays exhibiting a triangular shape with a clear predominance of the population on the B sublattice, opposite to that of the excitation beam. This polariton distribution resembles the wavefunction of electron for a single bulk vacancy in graphene [2, 3]. In contrast to the situation for a compressed lattice ($\beta = 2$), the polariton steady state is here spread over x and y directions. Note that Figure 3 of the main text is also presented in logarithmic scale. Fig. 3(b) shows the steady-state solution of Eq. (3) of the main text with the conditions: $E = E_0$, $t = 0.23$ meV, $\beta = 1$, and $\tau \approx 10$ ps.

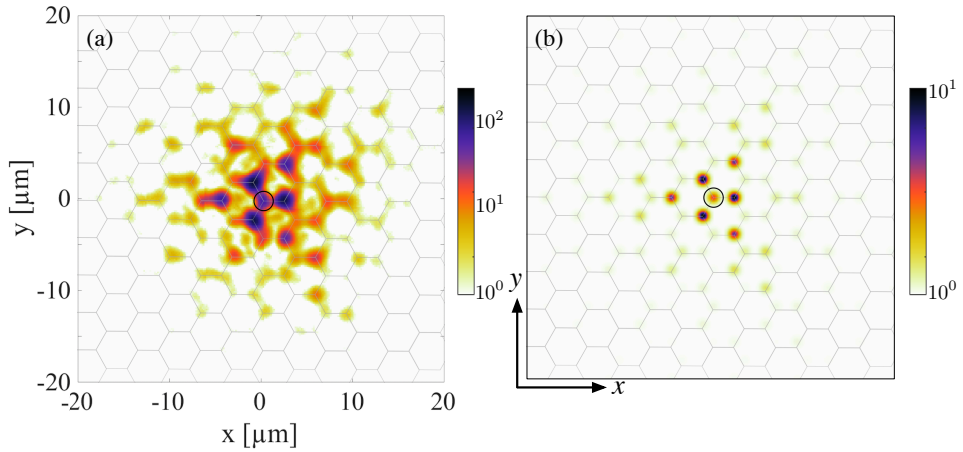

FIG. 3. All-optical analog of a vacancy state in a honeycomb lattice with $\beta = 1$. (a) Measured photoluminescence intensity in the real space at the energy of the Dirac point (E_0) when a single A-pillar is pumped (marked by a circle). (b) Steady-state solution of Eq. (3) of the main text when a single A-pillar is pumped at $E = E_0$ and considering $t = 0.23$ meV, $\beta = 1$, and $\tau \approx 10$ ps.

[1] C. Dutreix, L. Bilteanu, A. Jagannathan, and C. Bena, Friedel oscillations at the Dirac cone merging point in anisotropic graphene and graphenelike materials, Phys. Rev. B **87**, 245413 (2013).
[2] V. M. Pereira, F. Guinea, J. M. B. Lopes dos Santos, N. M. R. Peres, and A. H. Castro Neto, Disorder Induced Localized States in Graphene, Phys. Rev. Lett. **96**, 036801 (2006).
[3] T. O. Wehling, A. V. Balatsky, M. I. Katsnelson, A. I. Lichtenstein, K. Scharnberg, and R. Wiesendanger, Local electronic signatures of impurity states in graphene, Phys. Rev. B **75**, 125425 (2007).